arXiv:1009.3265v1 [astro-ph.CO] 16 Sep 2010

THE BULK OF THE BLACK HOLE GROWTH SINCE $z \sim 1$ OCCURS IN A SECULAR UNIVERSE: NO MERGER-AGN CONNECTION[*]

Mauricio Cisternas[1,19], Knud Jahnke[1], Katherine J. Inskip[1], Jeyhan Kartaltepe[2], Anton M. Koekemoer[3], Thorsten Lisker[4], Aday R. Robaina[1], Marco Scodeggio[5], Kartik Sheth[6,7], Jonathan R. Trump[8], René Andrae[1], Takamitsu Miyaji[9,10], Elisabeta Lusso[11], Marcella Brusa[12], Peter Capak[6], Nico Cappelluti[12], Francesca Civano[13], Olivier Ilbert[14], Chris D. Impey[7] Alexie Leauthaud[15], Simon J. Lilly[16], Mara Salvato[17], Nick Z. Scoville[6], and Yoshi Taniguchi[18]

[1] Max-Planck-Institut für Astronomie, Königstuhl 17, D-69117 Heidelberg, Germany
[2] National Optical Astronomy Observatory, 950 North Cherry Avenue, Tucson, AZ 85 721, USA
[3] Space Telescope Science Institute, 3700 San Martin Drive, Baltimore, MD 21218, USA
[4] Astronomisches Rechen-Institut, Zentrum für Astronomie der Universität Heidelberg, Mönchhofstr. 12-14, 69120 Heidelberg, Germany
[5] IASF-INAF, Via Bassini 15, I-20133 Milano, Italy
[6] California Institute of Technology, 1200 East California Boulevard, MC 249-17, Pasadena, CA 91125, USA
[7] Spitzer Space Center, California Institute of Technology, Pasadena, CA 91125, USA
[8] Steward Observatory, University of Arizona, 933 North Cherry Avenue, Tucson, AZ 85721, USA
[9] Instituto de Astronomía, Universidad Nacional Autónoma de México, Ensenada, México (PO Box 439027, San Diego, CA 92143-9027, USA)
[10] Center for Astrophysics and Space Sciences, University of California at San Diego, Code 0424, 9500 Gilman Drive, La Jolla, CA 92093, USA
[11] INAF-Osservatorio Astronomico di Bologna, via Ranzani 1, I-40127 Bologna, Italy
[12] Max-Planck-Institut für Extraterrestrische Physik, Giessenbachstrasse 1, D-85748 Garching bei München, Germany
[13] Harvard Smithsonian Center for Astrophysics, 60 Garden Street, Cambridge, MA 02138, USA
[14] Laboratoire d'Astrophysique de Marseille, BP 8, Traverse du Siphon, 13376 Marseille Cedex 12, France
[15] LBNL & Berkeley Center for Cosmological Physics, University of California, CA 94720, USA
[16] Department of Physics, ETH Zürich, CH-8093 Zürich, Switzerland
[17] Max-Planck-Institut für Plasmaphysik, Boltzmanstrasse 2, D-85741 Garching, Germany and
[18] Research Center for Space and Cosmic Evolution, Ehime University, Bunkyo-cho, Matsuyama 790-8577, Japan

ABSTRACT

What is the relevance of major mergers and interactions as triggering mechanisms for active galactic nuclei (AGN) activity? To answer this longstanding question, we analyze 140 *XMM*-selected AGN host galaxies and a matched control sample of 1264 inactive galaxies over $z \sim 0.3 - 1.0$ and $M_* < 10^{11.7} M_\odot$ with high-resolution *HST*/ACS imaging from the COSMOS field. The visual analysis of their morphologies by 10 independent human classifiers yields a measure of the fraction of distorted morphologies in the AGN and control samples, i.e. quantifying the signature of recent mergers which might potentially be responsible for fueling/triggering the AGN. We find that (i) the vast majority (>85%) of the AGN host galaxies do not show strong distortions, and (ii) there is no significant difference in the distortion fractions between active and inactive galaxies. Our findings provide the best direct evidence that, since $z \sim 1$, the bulk of black hole accretion has not been triggered by major galaxy mergers, therefore arguing that the alternative mechanisms, i.e., secular processes and minor interactions, are the leading triggers for the episodes of major black hole growth. We also exclude an alternative interpretation of our results: a significant time lag between merging and the observability of the AGN phase could wash out the most significant merging signatures, explaining the lack of enhancement of strong distortions on the AGN hosts. We show that this alternative scenario is unlikely due to: (i) recent major mergers being ruled out for the majority of sources due to the high fraction of disk-hosted AGN, (ii) the lack of a hidden X-ray signal in merging inactive galaxies as a signature of a potential buried AGN, and (iii) the low levels of soft X-ray obscuration for AGN hosted by interacting galaxies, in contrast to model predictions.

Subject headings: galaxies: active — galaxies: evolution — galaxies: interactions — quasars: general

1. INTRODUCTION

There is a general agreement that supermassive black holes (BHs) lie at the centers of nearly all galaxies, or at least those with a bulge component. Additionally, strong correlations exist between the BH mass and various properties of the galactic bulge, including luminosity (Kormendy & Richstone 1995; Magorrian et al. 1998), stellar velocity dispersion (Gebhardt et al. 2000; Ferrarese & Merritt 2000; Tremaine et al. 2002), and stellar mass (Marconi & Hunt 2003; Häring & Rix 2004). While it has been recently proposed that these correlations are just the product of a statistical convergence of several galaxy mergers over cosmic

time (Peng 2007; Jahnke & Maccio 2010), these correlations have often been interpreted as the signature of coupled evolution between the BH and its host galaxy (Kauffmann & Haehnelt 2000; Volonteri et al. 2003; Wyithe & Loeb 2003; Granato et al. 2004; Hopkins et al. 2007; Somerville et al. 2008).

Given that most galaxies are believed to have undergone a quasar phase, and that the central BH represents a relic of this event (Lynden-Bell 1967; Richstone et al. 1998), the co-evolution picture is naturally very appealing even while some aspects of it remain unclear. It has been suggested that most of the mass of the BH is built up during the brightest periods of this quasar phase (Soltan 1982; Yu & Tremaine 2002). If there is such a connection between the growth of the BH and its host galaxy, periods of quasar activity should occur alongside the growth of the bulge, and the mechanism that triggers the accretion onto a once quiescent BH, turning it into an active galactic nucleus (AGN), should be tightly linked with the overall evolution of the host galaxy. The nature of AGN triggering is therefore of key importance for our understanding of galaxy evolution in general.

According to the current paradigm of hierarchical structure formation, major mergers are a crucial element in the assembly and growth of present-day galaxies (e.g., Kauffmann et al. 1993; Cole et al. 2000; Somerville et al. 2001; Bell et al. 2006; Robaina et al. 2010). A closer look into the behaviour of simulated collisions between galaxies, beginning with the pioneering work of Toomre & Toomre (1972), suggests that gravitational interactions are an efficient way of transporting material towards the very center of a galaxy. Mergers and strong interactions can induce substantial gravitational torques on the gas content of a galaxy, depriving it of its angular momentum, leading to inflows and the build up of huge reservoirs of gas in the center (Hernquist 1989; Barnes & Hernquist 1991, 1996; Mihos & Hernquist 1996; Springel et al. 2005; Cox et al. 2006; Di Matteo et al. 2007; Cox et al. 2008).

From early on, major mergers have been related to observations of powerful nuclear starbursts (Gunn 1979), and connections with quasar activity were made soon after. Stockton (1982), in a study of luminous quasars with close companions, suggested that these neighboring galaxies could be survivors of a strong interaction with the quasar. Further observational studies came to support this picture: more cases of quasars with close companions were found, and post merger features were detected in the host galaxies, whenever it was possible to resolve them (e.g., Heckman et al. 1984; Gehren et al. 1984; Hutchings et al. 1984, 1988; Stockton & Ridgway 1991; Hutchings & Neff 1992). The merger-quasar connection scenario gained strength with the discovery of the ultraluminous infrared galaxies (ULIRGs). More than 95% of these were found in a merging state, some of them hosting an AGN. This led to the scenario in which ULIRGs and quasars were part of a same chain of events (Sanders et al. 1988a,b; Sanders & Mirabel 1996; Surace et al. 1998; Surace & Sanders 1999; Surace et al. 2000; Canalizo & Stockton 2000, 2001).

With the advent of the *Hubble Space Telescope* (*HST*), deep imaging of AGN host galaxies at higher redshifts became possible with unprecedented resolution. Many observational studies of quasars found a high rate of merg-

ing signatures in their hosts and detected the presence of very close companions, which before *HST* could not be resolved (e.g., Bahcall et al. 1997; Canalizo & Stockton 2001; Zakamska et al. 2006; Urrutia et al. 2008). At the same time, deeper imaging of quasar host galaxies that were initially classified as undisturbed, revealed post-merger features not previously detected, both from space- (Canalizo et al. 2007; Bennert et al. 2008) and ground-based observations (Ramos Almeida et al. 2010).

There is, however, one major caveat for the studies listed above: none of them made use of, or had the access to, an appropriate control sample of inactive galaxies; such a control sample is essential for discerning if the merger rate is in fact enhanced with respect to the "background level", i.e., the merger rate of inactive galaxies. Only Dunlop et al. (2003) compared their statistically complete sample of quasars against the quiescent galaxy population, finding no difference in the structural parameters between samples, as well as no enhancement in the large scale disturbances. Even if not explicitly, this showed a clear divergence from previous studies regarding the merger-AGN connection scenario.

A new era of large *HST* programs now offers the potential for resolving this discrepancy. The imaging of larger, contiguous fields has yielded a large number of objects, making it possible to study AGN hosts at space-based resolution, and at the same time to compile a control sample of non-active galaxies. Initial studies using *HST* imaging by Sánchez et al. (2004) with the Galaxy Evolution from Morphologies and SEDs survey (GEMS, Rix et al. 2004) and by Grogin et al. (2005) with the Great Observatories Origins Deep Survey (GOODS, Giavalisco et al. 2004) found no evidence for an enhancement in merging signatures of AGN hosts over control galaxy samples. If merger activity does not play a major role in AGN triggering, other methods to produce gas inflows and fuel the BH could also be of importance. Alternate mechanisms—minor interactions, large scale bars, nuclear bars, colliding clouds, supernova explosions—can also lead to angular momentum removal and gas inflows from different scales to the central regions (for reviews, see Wada 2004; Martini 2004; Jogee 2006). While these mechanisms haven usually been related to Seyfert galaxies and low-luminosity AGN (e.g., Simkin et al. 1980; Taniguchi 1999; Hopkins & Hernquist 2009), they could potentially play a larger role than usually reckoned for more luminous quasars as well. Although these are intriguing results, the field sizes of 0.25 deg^2 and 0.08 deg^2 respectively were still too small for definitive conclusions to be drawn. A suitably larger sample would be required to turn these appealing hints into statements.

In this context, we tackle this long-standing issue by performing a comprehensive morphological analysis of a sample of X-ray selected AGN host galaxies from the Cosmic Evolution Survey (COSMOS, Scoville et al. 2007b), the largest contiguous area ever imaged with the *HST* (Scoville et al. 2007a; Koekemoer et al. 2007). Our goal is to disentangle the actual relevance and predominance of major galaxy mergers from the other suggested mechanisms for the fueling of the BH.

In the past, targeted high-resolution imaging of quasar hosts has only been possible for small samples, while extensive ground-based surveys with large samples have lacked of the necessary resolution to perform detailed

morphological studies at moderate redshifts. Earlier results from the detailed analysis by Gabor et al. (2009), where the morphologies of $\sim$400 AGN host galaxy candidates from the COSMOS field where parametrized, showed that these had an asymmetry distribution consistent with that of a control sample of inactive galaxies, and lacked an excess of companions, already suggesting that major interactions were not predominant among AGN as a triggering mechanism. Here we use the largest sample of optically confirmed X-ray selected AGN ever imaged at *HST* resolution from the COSMOS survey, and perform a visual inspection of the morphologies of the host galaxies. We opt for visual analysis of our galaxies over an automatic classification system because of the inherent problems and incompleteness of the latter in identifying mergers, even for some obvious cases (e.g., Jogee et al. 2009). To establish the relevance of our findings, we compare the AGN hosts to a matching sample of inactive galaxies from the same exact dataset.

Throughout this paper we assume a flat cosmology with $H_0 = 70$ km s^{-1} Mpc^{-1}, $\Omega_M = 0.3$, and $\Omega_\Lambda = 0.7$. All magnitudes are given in the AB system unless otherwise stated.

2. DATASET AND SAMPLE

Our sample consists of a complete subsample of X-ray selected type–1 and type–2 AGN from the COSMOS field.

The COSMOS survey features the largest contiguous area ever imaged with the *HST*. The location of the 1.64 deg^2 field, close to the celestial equator, allows access from several major space and ground based observatories, enabling a large multiwavelength coverage from X-ray to radio from supplementary observational projects.

One of the most effective ways of finding AGN is to make use of the X-ray emission from the accreting BH. Complete coverage of the whole COSMOS field in X-rays was achieved with the *XMM-Newton* (XMM-COSMOS, Hasinger et al. 2007; Cappelluti et al. 2009) through 55 pointings with a total exposure time of $\sim$1.5 Ms. We use the catalog presented in Brusa et al. (2010), which provides the most likely optical and infrared counterparts to the *XMM* sources based on a likelihood ratio technique (see Brusa et al. 2007 for details).

From the X-ray catalog we draw a subsample of sources classified as type–1 AGN from spectroscopic surveys (Trump et al. 2007, 2009; Lilly et al. 2007) revealing broad emission lines, and from spectral energy distribution (SED) fitting (Capak et al. 2007; Salvato et al. 2009; Ilbert et al. 2009). We also include a subsample of X-ray selected type–2 AGN which feature narrow emission lines in their spectra, based on the sample used by Gabor et al. (2009). We refine this subsample by cross checking with the latest optical counterparts presented in Brusa et al. (2010).

In this paper, we analyze the morphological properties of the AGN host galaxies. For this, we take advantage of the high resolution imaging of the COSMOS field with the *HST*. These observations comprise 583 orbits using the Advanced Camera for Surveys (ACS) with the F814W (broad *I*-band) filter (Koekemoer et al. 2007). The imaging data feature an oversampled scale of 0$\farcs$03/pixel. Although the ACS survey of the COSMOS field is highly homogeneous, the exact depth achieved is
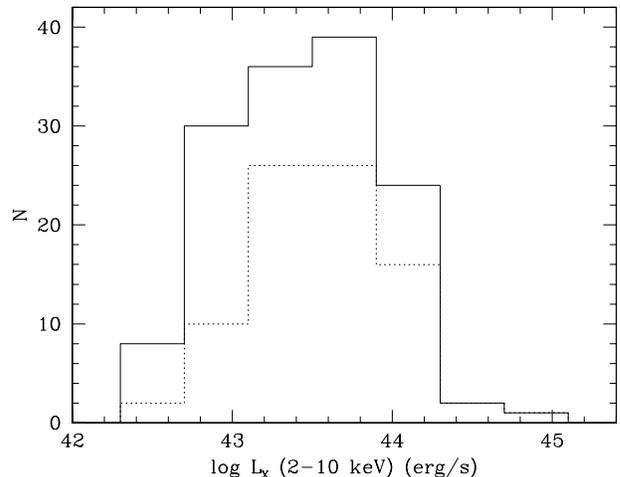
Figure 1. The X-ray luminosity distribution of our subsample in the 2-10 keV energy band (solid line). For reference, we also show the distribution of the type–1 AGN subsample only (dotted line).

dependent on the angle of the telescope with the Sun at the time of the observations (Leauthaud et al. 2007). 96 out of the 575 pointings were made with an angle smaller than a critical value of 70°, leading to a slightly shallower image. The limiting surface brightness levels above the background for the pointings made with an angle with the Sun larger and smaller than the critical value are $\sim$23.3 mag arcsec^{-2} and $\sim$22.9 mag arcsec^{-2} respectively.

We restrict our sample to the redshift range $z \sim 0.3 - 1.0$. For the majority of our final sample, we used high-confidence spectroscopic redshifts, while for the rest (20%), we used photometric redshifts by Salvato et al. (2009). The lower redshift cut is chosen due to the low number of AGN below $z \sim 0.3$ (see Section 3 for further details), and also to avoid working with saturated sources. The upper limit arises because the F814W filter is shifted into restframe-UV for sources above $z \sim 1$. This would mean that we would be specifically looking at the light from young stars and star formation knots, and therefore at biased morphologies. At the same time, the quasar would start to dominate due to its blue color strongly outshining the host, and for the case of the type–1s, making it impossible to resolve.

Given our interest in the morphologies of our sample of AGN host galaxies, we decided not to consider galaxies fainter than $I_{F814W} = 24$. Visual morphological classification of these objects would be particularly difficult, and we determined that no consistent information could be extracted at this magnitude. For the case of the type–1 sample, we applied this criterion *after* the nucleus removal (see Appendix A for details).

This selection yields 83 type–1 and 57 type–2 AGN.

Figure 1 shows the X-ray luminosity distribution of our sources in the 2-10 keV energy band. The values were obtained mainly from those calculated by Lusso et al. (2010) and are complemented with those by Mainieri et al. (2007). The median of our distribution lies at $L_X = 10^{43.5}$ erg s^{-1}, which means that we are probing a reasonably luminous representative AGN sample. For reference, in Figure 1 we also show the X-ray luminosity distribution of the type–1 AGN sample

only, which dominates the overall distribution and has a slightly brighter median L_X ($10^{43.6}$ erg s^{-1}) in comparison to the type–2 sample ($10^{43.3}$ erg s^{-1}).

3. METHODOLOGY

In this paper we analyze the morphologies of a sample of AGN host galaxies and of a control sample of inactive galaxies using high-resolution HST/ACS single I-band images. In the following subsections we explain how we built the comparison sample, the motivation of choosing a visual inspection over an automatic method, and the classification scheme used.

Analyzing the host galaxies of type–1 AGN is complex, due to the presence of the bright active nucleus in the images, that, depending on the contrast, can outshine the host galaxy to different extents. We overcome this issue through a two-dimensional decomposition of the quasar and its host galaxy, modeling the quasar with a point spread function (PSF) and the host galaxy with a Sersic (1968) profile using GALFIT (Peng et al. 2002, 2010), and then removing the nuclear contribution. This process is described in detail in Appendix A.

3.1. *Comparison Sample*

The large number of galaxies available from the COSMOS HST observations provides us with the unique possibility of building a control sample from the same dataset that we draw our AGN from. While we cannot construct a genuine stellar mass-selected sample of galaxies, due to the lack of color information for the quasar hosts at the ACS resolution, our comparison galaxies are chosen to match individual AGN hosts both in apparent magnitude in the F814W filter and in photometric redshifts. This is sufficient since the redshift and brightness determine the signal-to-noise (S/N), which is the most important parameter for analyzing visual morphologies and identifying merger signatures. Meanwhile the stellar mass dependence on the merger rate is, at best, weak (Jogee et al. 2009).

Specifically, for each AGN host galaxy, we select 10 similar comparison galaxies from the COSMOS ACS catalog (Leauthaud et al. 2007). Each selected comparison galaxy is required to have a I-band magnitude within a range of $\triangle I_{F814W} = 0.1$, and a photometric redshift within a range of $\triangle z = 0.05$. If not enough galaxies were found, the search ranges were increased by 10%. On average, 1.8 iterations were performed to find the required number of inactive galaxies for each AGN host. For the case of the type–1 AGN subsample, the magnitudes of the host galaxies after the removal of the quasar are used for the selection of the control sample.

With the inactive comparison sample in hand, we remove galaxies that are unlikely to be AGN host galaxy counterparts *a priori* via an initial visual inspection. Such galaxies include: (1) bulgeless disks and irregulars, which would represent a low mass population, having no corresponding partners on the AGN sample, and (2) for the type–1 sample, edge-on disks, which could in principle hold an AGN but this would be heavily obscured and therefore not be a type–1.

Finally, the construction of the control sample for the type–1 AGN requires an additional effort. The AGN removal process usually leaves residuals in the center which certainly affect any blind classification, making the quasar host galaxies readily discernible from the control sample. To resolve this problem, we mock up our selected inactive galaxies as AGN by adding a star in the center as a fake active nucleus, as we describe in Appendix B. We then apply the same subtraction procedure as for the original type–1 AGN, attempting to make the two samples indistinguishable. As we show in Appendix C, any effects on the selection of the comparison sample due to flux variations caused nucleus subtraction can be neglected.

Our final comparison sample consists of 1264 galaxies in total.

3.2. *Visual Classification*

Merger events come in many different flavors due to the large parameter space involved (e.g., merger stage, viewing angles, mass ratio, gas fractions). Sometimes they can be obvious at first sight, but some others can be very subtle, or simply undetectable at the sensitivity of the observations. At our redshift range and image resolution, it has been shown that automatic classification methods miss several obvious cases, and therefore cannot compete with visual inspection (Jogee et al. 2009). On the other hand, when the numbers involved are over the tens of thousands, visual classification becomes impractical[3] and an automatic approach would be needed. General measurements of structural parameters that can be correlated with some physical process have proven to be a good compromise (e.g, Reichard et al 2009, using the lopsidedness as a tracer of merging and star formation).

Considering the above, in this paper we opt to identify merger and interaction signatures visually. The number of objects we are dealing with allows us to do so ($\sim$1400 in total), and the image quality deserves a detailed case-by-case examination.

These visual studies can be subjective. The absolute merger fraction measured by visual classifiers will depend on their own experience and background. Nevertheless, if we instead consider the differential *between* the fractions of active and inactive galaxies, this subjectiveness can be accounted for. Furthermore, the consistency of this study is improved by (1) using ten independent human classifiers to add statistical robustness, and (2) mixing both samples of active and inactive galaxies so that the classification is actually blind, and therefore does not favor either the AGN hosts or the inactive galaxies.

We break the classification down to two parameters:

1. *Hubble type* – We attempt to state whether the host galaxy belongs to one of the two basic morphological classes: bulge- or disk-dominated.

2. *Distortion class* – We define 3 classes regarding the degree of distortion of the galaxy:

   - *Dist-0* – Galaxies that appear undisturbed, smooth and/or symmetric, showing no interaction signatures. This also applies to cases where the small diameter of the galaxy does not allow a detailed analysis. We pay particular attention to self-induced asymmetries such as dust lanes or star forming regions,

---

[3] With the notable exception of the citizen-based Galaxy Zoo project (Lintott et al. 2008, http://www.galaxyzoo.org).

Table 1
Results from the visual analysis by the 10 classifiers.

Classifier	MC	KI	KJ	JK	AK	TL	AR	MS	KS	JT	μ
N_{AGN}	140	140	140	140	22	40	57	140	38	98	-
N_{type-1}	83	83	83	83	22	40	0	83	19	41	-
N_{type-2}	57	57	57	57	0	0	57	57	19	57	-
N_{CS}	1264	1264	1264	1264	177	357	537	1264	357	903	-
Hubble type											
$Bulge_{AGN}$	25.7%	51.4%	31.4%	20.0%	40.9%	55.0%	29.8%	43.6%	26.3%	37.8%	35.2% ± 11.0%
$Disk_{AGN}$	74.3%	48.6%	68.6%	80.0%	59.1%	45.0%	70.2%	56.4%	73.7%	62.2%	64.8% ± 11.0%
$Bulge_{CS}$	24.6%	43.3%	29.6%	25.2%	47.5%	54.3%	29.4%	43.6%	17.9%	40.5%	34.3% ± 9.5%
$Disk_{CS}$	75.4%	56.7%	70.4%	74.8%	52.5%	45.7%	70.6%	56.4%	82.1%	59.5%	65.7% ± 9.5%
Distortions											
Dist–0_{AGN}	62.9%	43.6%	48.6%	56.4%	50.0%	47.5%	71.9%	56.4%	47.4%	55.1%	54.2% ± 7.5%
Dist–0_{CS}	65.5%	47.3%	60.1%	63.0%	67.8%	51.5%	78.0%	58.5%	51.5%	61.2%	59.9% ± 7.6%
Δ_{Dist-0}	-2.6%	-3.7%	-11.6%	-6.5%	-17.8%	-4.0%	-6.1%	-2.1%	-4.2%	-6.1%	-5.6% ± 3.5%
Dist–1_{AGN}	24.3%	26.4%	45.0%	32.9%	40.9%	40.0%	21.1%	30.0%	50.0%	16.3%	30.8% ± 9.3%
Dist–1_{CS}	22.4%	28.3%	34.2%	26.9%	19.2%	34.2%	16.0%	33.5%	39.2%	17.8%	27.5% ± 6.5%
Δ_{Dist-1}	1.9%	-1.9%	10.8%	6.0%	21.7%	5.8%	5.0%	-3.5%	10.8%	-1.5%	3.2% ± 5.7%
Dist–2_{AGN}	12.9%	30.0%	6.4%	10.7%	9.1%	12.5%	7.0%	13.6%	2.6%	28.6%	15.0% ± 8.8%
Dist–2_{CS}	12.1%	24.4%	5.7%	10.1%	13.0%	14.3%	6.0%	7.9%	9.2%	20.9%	12.6% ± 6.5%
Δ_{Dist-2}	0.8%	5.6%	0.7%	0.6%	-3.9%	-1.8%	1.1%	5.7%	-6.6%	7.6%	2.4% ± 3.5%

Note. — We indicate the number of objects classified by each person, for the AGN sample and individually for each subsample (type–1 and type–2), as well as for the comparison sample (CS). For the distortion classifications, we include the difference between samples as Δ_{Dist-X}=Dist–X_{AGN} – Dist–X_{CS}. For each category we include the mean, μ, and its dispersion, weighted according to the number of objects classified by each person.

which are usually seen as small clumps in well-resolved spirals.

- *Dist-1* – Here we include objects with mild distortions. This could be due to a minor merger for example, but at the same time could also be because of low S/N. This interaction class is a "gray zone" in which most of the discrepancies in the classification between the 10 people arise.
- *Dist-2* – Strong distortions, potential signs for ongoing or recent mergers. This class mainly includes galaxies which have highly disturbed morphologies or show visible signatures of strong interactions, such as large tidal tails, arcs, debris, etc. Double nucleus systems also fall into this category.

For the visual inspection, the classifiers had access to FITS images which they could re-scale in order to look for high-contrast and subtle features that may have not showed up at an arbitrary brightness scale.

4. RESULTS

The results from the visual classification by ten people (MC, KI, KJ, JK, AK, TL, AR, MS, KS, JT), for both Hubble type and distortion classes, are shown in table 1. For the different distortion classes, we show the difference between samples (hereafter Δ) as the distortion fraction of the AGN minus that of the control sample. The results are weighted according to the number of objects classified by each person[4], and used to calculate the mean fractions, μ, which we also display in table 1. Figures 2 and

[4] Each classifier looked at a minimum of ~200 galaxies from the combined sample. For each classifier the samples were shuffled, to assure that even if all of them decided to look at 200 galaxies, they

Table 2
Testing our Hubble type classification

	μ[a]	GALFIT[b]	ZEST[c]
$Bulge_{AGN}$	35.2%	25.7%	-
$Disk_{AGN}$	64.8%	55.0%	-
$Bulge_{CS}$	34.3%	41.2%	19.6%
$Disk_{CS}$	65.7%	43.5%	67.8%

[a] Weighted mean of the 10 classifications (as in table 1).
[b] Percentages over 100% of the samples. The rest of the objects had an intermediate Sérsic index.
[c] Percentages over 100% of the comparison sample. The remaining galaxies were classified as irregulars (11.3%) by ZEST, and a few did not make it to the catalog (1.2%).

3 show examples of active and inactive galaxies which were classified with 100% agreement, arranged into the different Hubble type and distortion classes respectively.

4.1. *Perception of the Hubble type*

No morphology priors are applied in the selection of our comparison sample, with the minor exception of the pruning of irregulars and edge-on disks as described in Section 3.1. In order to test whether the samples are consistent regarding their morphological composition, we compare the AGN and comparison samples in table 1. Although the mean values show a high dispersion due to the large discrepancies between classifiers, the results for the AGN and comparison samples are in good general agreement for each classifier.

The large fraction of disks in both samples is interesting. To verify if this could be due to systematic bias by

would be looking at different objects. On average, each galaxy was classified 6.3 ± 1.0 times.
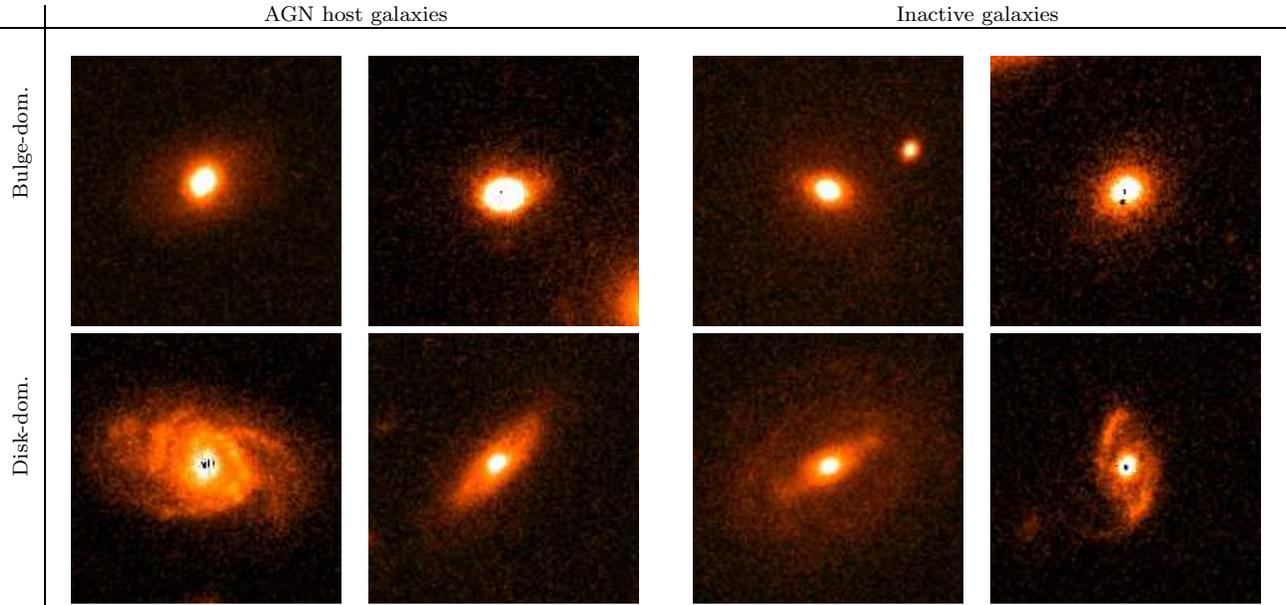
Figure 2. Example galaxy images arranged into different morphological classes with 100% agreement between the independent classifiers. The cutouts are $4\rlap{.}''8 \times 4\rlap{.}''8$. Black residuals at the center of some of the galaxies are residuals from the point source removal.

the classifiers, we will use two independent parametric estimators of the morphological type available at hand. First we compare the results from our GALFIT models chosen earlier, which we extended to our type–2 sample as well as to its comparison galaxies. We identify sources as bulge- or disk-dominated if the best-fit results from GALFIT had Sérsic indices of $n = 4$ and $n = 1$ respectively. The rest of the galaxies fell between the two. As a second test, we look up the results for our comparison sample from the Zurich Estimator of Structural Types (ZEST, see Scarlata et al. 2007 for details), in which the structure of thousands of COSMOS galaxies was quantified through a principal component analysis over a combination of Sérsic index and 5 non-parametric diagnostics. The ZEST results show the fractions of galaxies classified either as bulges or disks. Of the remaining fraction classified as neither, the majority (11.3%) were classified as irregulars, most likely due to the lack of sensitivity of these automatic classification schemes to peculiar systems such as interacting galaxies; this is consistent with the observed fraction of highly distorted comparison galaxies. Sixteen galaxies, accounting for the remaining 1.2%, did not make it into the catalog.

Table 2 shows both of these tests along with the weighted mean fractions for comparison. It is clear that the numbers from these tests follow the trend seen in the visual classification. These tests provide a lower limit to the fraction of disks, with $> 50\%$ of our samples being hosted by true disks.

4.2. *The distortion fractions*

Our prime interest lies in the observed difference in distortion fractions *between* samples of active and inactive galaxies. The absolute values in distortion fractions determined by the 10 classifiers are of lesser interest since the internal calibration for the three distortion classes differs between the classifying individuals. Since any subjectiveness will be applied equally to both active and inactive samples, using the differences in the distortion

fractions instead of absolute levels removes the person-to-person calibration differences and allows an unbiased interpretation.

Considering that the merging signatures we were looking for could sometimes be faint and weak, we address the potential loss of sensitivity to such features due to the slightly shallower limiting magnitudes for $\sim 17\%$ of the pointings (i.e. those with sun-angles of $< 70°$). For each person, we have also carefully analyzed the results by dividing their classified sample into sources with sun-angles either side of this critical angle. We find that there is no statistically significant difference in the distortion fractions as a function of sun-angle. In addition, as the assignment of individual objects to either a deep or shallow field is effectively random, and given that the AGN distortion fractions are compared directly with those of a comparison sample selected from the same dataset (and thus with the same limiting surface brightness issues), the overall impact on our results of any bias towards smaller distortion fractions in the shallower fields would in any case be negligible.

The objects that fell into the Dist-2 class were those which presented the strongest distortions, and hence signatures of a major interaction, for each individual classifier As any difference in recent major merger incidence would show itself in this class, we will focus on the Dist-2 results here.

4.2.1. *Combining 10 classifications*

In table 1 we have already listed the Dist-2 fractions for all classifiers, their mean values, and also the mean of the difference in Dist-2 fractions between the AGN and comparison samples. This permits the following initial assessment under the assumption of Gaussian errors: the difference (2.4%) is below the uncertainty of 3.5%, and hence it is not significant.

Nevertheless, since the error distribution is in fact *not* Gaussian but follows a *binomial* distribution (according to the number of distorted galaxies in a sample of given
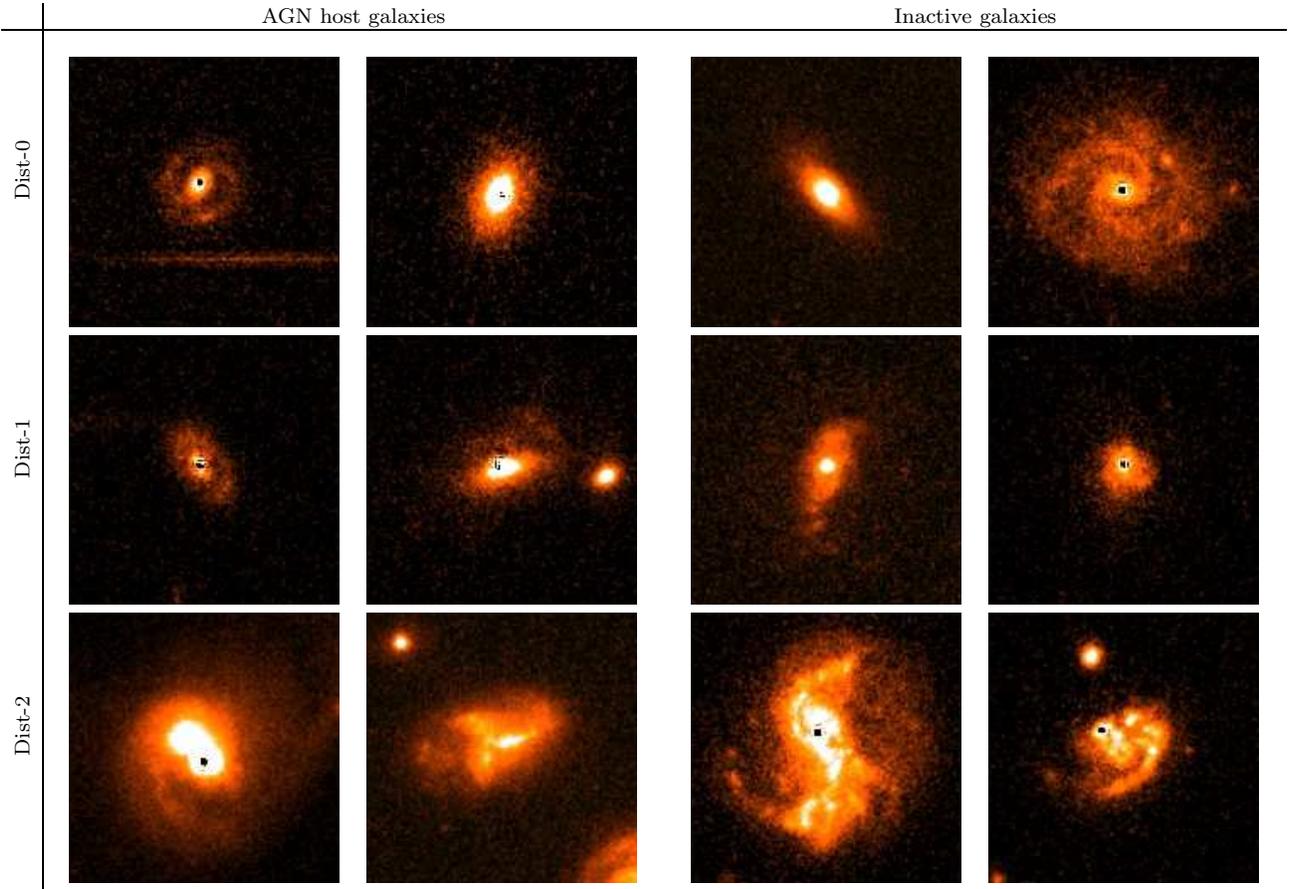
Figure 3. Example galaxy images arranged into different distortion classes with 100% agreement between the independent classifiers. The cutouts are $4''8 \times 4''8$. Black residuals at the center of some of the galaxies are residuals from the point source removal.

size) it is important that we use the correct combination of results in order to give answers to the two main questions: (i) Is there a genuine difference between the fractions of strongly distorted AGN hosts and inactive galaxies, and (ii) with the given sample size, what difference in distortion fractions between samples can we actually rule out at a given confidence level—in this case we chose 95%. The first question asks whether the given dataset shows an enhanced AGN distortion fraction or not. The second question probes the discriminative power of this sample, and allows us to gauge the actual importance of a null-result in question (i), since a decreasing sample size means an increasing uncertainty in the distortion fractions and hence small samples have near zero discriminative power.

Using the correct binomial error statistics for the distortion fractions of AGN and inactive galaxies, we compute for each classifier the probability distribution for the difference Δ_{Dist-2}. This is done by randomly sampling the binomial distributions for distorted AGN and inactive galaxies one million times each, i.e., sampling Dist-2_{AGN} and Dist-2_{CS} for each classifier, and taking the difference. Afterwards we normalize the distributions by the absolute fraction of distortions on the control sample for a given classifier, that is, by the Dist-2_{CS} values measured by each person as shown in table 1. This yields Δ_{Dist-2}/Dist-2 in units of absolute distortion fraction (Figure 4). At this point, these distributions from all 10 classifiers can then be combined in "differential" space,

where we are insensitive to between-person scatter. We combine them by coadding their histograms, weighted by the size of the sample each person classified[5].

The resulting probability distribution is shown in Figure 5. The histogram is fully consistent with zero difference, as indicated by the central 68% confidence interval denoted by the vertical dashed lines estimated by the areas at both ends, encompassing 16% each. This confirms the simple analysis from above: our study shows no significant difference between the fractions of strong distortions of AGN and inactive galaxies. Regarding the discriminative power of our sample, in Figure 6 we show the cumulative distribution of the Dist-2_{AGN} fraction from Figure 5. The distribution shows that with 95% confidence the distortion fraction of AGN is in any case not larger than the inactive distortion fraction by a factor of 1.9, when considered relative to the mean distortion level found by the 10 classifiers (12.6%). Hence, the vast majority of AGN host galaxies at $z < 1$ with the given luminosities do not show signatures of having experienced a recent major merger.

4.2.2. Mass dependency

Even if there is no overall difference in the fractions of highly distorted galaxies, there is still the possibility that an enhancement of the AGN merger fraction could

[5] This represents a combined Bayesian posterior probability distribution with sample sizes as individual priors.
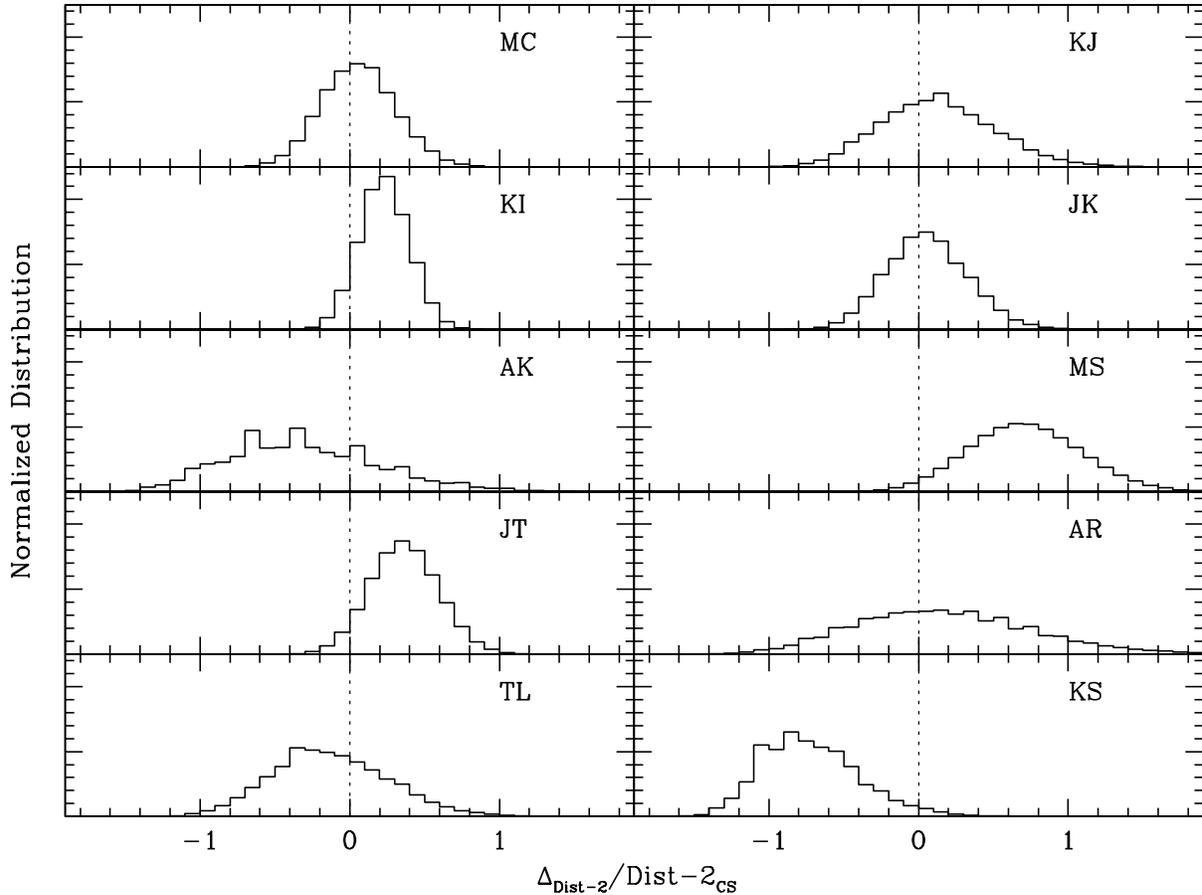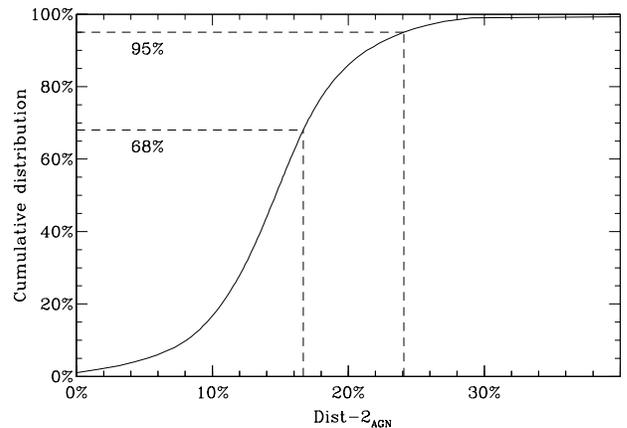
Figure 4. Distributions of the difference in the fraction of highly distorted galaxies between the AGN and control samples for the 10 classifiers. A deviation from zero difference (dotted line) towards positive values indicates a higher fraction of distorted active galaxies, whereas a higher fraction of distorted inactive galaxies tend to more negative values.
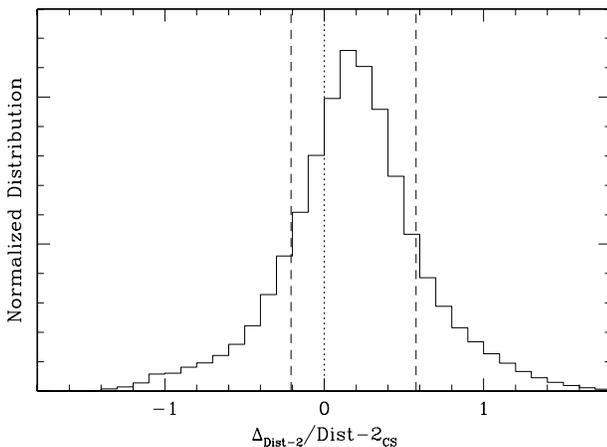

Figure 5. Combined posterior probability distribution of the difference of highly distorted galaxies between the AGN and control sample for the 10 classifiers. The central 68% confidence level is marked with vertical dashed lines, which shows that the histogram is consistent with zero difference (dotted line), ruling out any significant enhancement of merging signatures on our sample of AGN hosts with respect to the comparison sample of inactive galaxies.

Figure 6. Cumulative distribution of the simulated Dist-2_{AGN} fractions, showing the 68% and 95% confidence levels with the dashed lines. As mentioned in the text, this confirms with a 95% confidence that the highly distorted AGN fraction can *not* be larger than 24.08%.

be *hidden* because we consider the sample as a whole, regardless of stellar mass. Although the merger fraction is expected to be roughly constant as a function of mass (Jogee et al. 2009), major merging is a key element

in the assembly and evolution of massive galaxies (e.g., Bell et al. 2006; Lin et al. 2008; van der Wel et al. 2009; Robaina et al. 2010). In order to test if the fraction of highly distorted AGN host galaxies is significantly enhanced at the massive end (higher than $\sim 10^{10.5}\ M_\odot$), we have estimated stellar masses for our samples of active and inactive galaxies. We use the calibration from
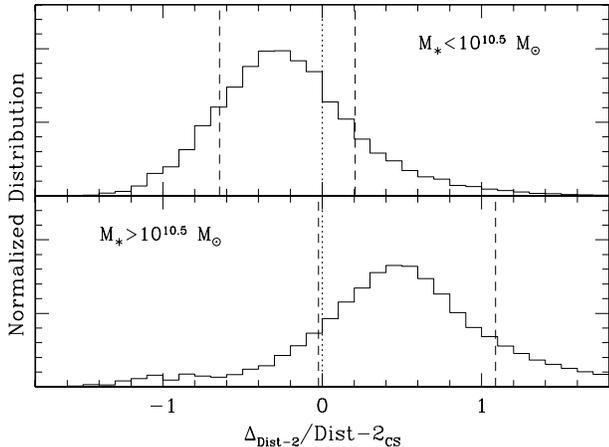
Figure 7. The combined differences in distortions of intermediate ($10^{9.3} < M_*/M_\odot < 10^{10.5}$; top panel) and massive ($10^{10.5} \leq M_*/M_\odot < 10^{11.7}$; bottom panel) galaxies are shown. In both cases, the central 68% confidence levels (dashed lines) are consistent with zero (dotted line).

Bell & de Jong (2001) based on the Chabrier IMF. By obtaining the V-band luminosities:

$$L_V = 10^{-0.4(V-4.82)} \qquad (1)$$

and assuming a common mass-to-light ratio from the rest-frame $(B-V)$ color, we derive stellar masses in solar units:

$$M_* = 10^{-0.728+1.305(B-V)} \times L_V \qquad (2)$$

with all magnitudes in Vega zero-point.

For the inactive galaxies and the type–2 subsample we obtain rest-frame B and V from the photometric catalog by Ilbert et al. (2010). For the type–1 AGN, however, we cannot use that information because it includes the contribution from the luminous quasar. Therefore, we obtain the rest-frame V-band luminosities from the observed I_{F814W} after the nucleus removal process, and estimate the color term by computing the linear regression over the restframe $(B - V)$ colors as a function of redshift for the type–2 AGN. This yields the relation

$$(B - V)_{Vega} = 0.136\ z + 0.541. \qquad (3)$$

The combined differences of highly distorted galaxies for 2 bins of stellar mass ($10^{9.3} - 10^{10.5} M_\odot$ and $10^{10.5} - 10^{11.7} M_\odot$) are shown in Fig 7. For both samples the ratio of galaxies occupying the massive bin is roughly 2:1 relative to the less massive one. Even if there is a modest increment in the difference between samples in favor of the AGN hosts for stellar masses higher than $\sim 10^{10.5}\ M_\odot$, it is again within the 68% error, i.e., it is not statistically significant. Therefore, it cannot be considered as an empirical proof of an enhancement at the massive end.

5. DISCUSSION

From a detailed analysis of the results of our visual classification we showed that the fractions of heavily distorted active and inactive galaxies are consistent within the central 68% confidence interval, and that the Dist-2 fraction of AGN host galaxies is less than twice that of the inactive galaxies at a 95% significance level, as shown in Figures 5 and 6 respectively. Putting these findings in

context, provided that the duration of merger signatures and the visibility of the AGN phase overlap with each other, this indicates that there is no evidence that major merging plays a key role in the triggering of AGN activity in our sample. But what of the possible alternative scenario in which, in spite of a causal connection between merging and AGN triggering, we do not detect an enhancement of merger signatures in the AGN population due to a significant time lag between the interaction and the start of the quasar phase? Below we address this possible alternative interpretation with some simple tests, and discuss the implications of our results.

5.1. *Alternative interpretation: time lag between merging and the observability of the AGN phase*

Appealing simulations of mergers between gas-rich galaxies state that the peak of star formation and quasar activity will occur during the final stages of the interaction, close to coalescence, within a more relaxed than distorted bulge-like remnant (Di Matteo et al. 2005; Springel et al. 2005). In these models, during the first passage only modest starbursts are triggered and no major BH accretion occurs, and therefore the galaxies would not be detected as AGN. Furthermore, *ad hoc* models that include obscuration in galaxy mergers (Hopkins et al. 2005b) predict that, beginning from the early stages of the interaction, the quasar is "buried" for $\sim$90% of its lifetime by large column densities, only revealing itself towards the end of the merger. However, all these models work with sub-grid prescriptions of BH accretion and fail to spatially resolve the actual accretion process by several orders of magnitude.

If there is indeed a substantial time lag after merging prior to the AGN activity becoming detectable, then the strong merging signatures we attempt to find could have already been washed out. Moreover, if quasars are obscured as the interacting galaxies coalesce, there could be a "contamination" population of undetected AGN activity occurring within our control galaxies undergoing a major merger. Finally, a third issue related to the obscuration plus time lag scenario is that the observed interactions that are occurring on a fraction ($\sim$15%) of our AGN host galaxies should be unrelated to the detected BH accretion—under the assumption of a large time lag we would not expect to see strong merging signatures.

5.1.1. *AGN hosted by disks: not a relic from a major merger*

In the preceding text we raised a possible caveat, that most major mergers could be missed because the time lag between merging and the observed quasar episode could be substantial, washing out the signatures that the *HST*/ACS resolution allows us to detect.

Models can provide us with some clues about the observability timescales during an interaction. For example, simulations of major mergers by Lotz et al. (2008) quantified that the strong signatures could still be detected 0.7 Gyr after the merger, by degrading their snapshots to the resolution of *HST* $z \sim 1$ imaging. Thus, in order to explain the observed zero distortion enhancement, a lag of at least 0.7 Gyr between coalescence and the visible phase of the AGN would be required for all galaxies[6]. It is, however, not straightforward to rely on

---

[6] For example, see Schawinski et al. (2010) who make an ex-

these studies to discard the time lag issue; given the large number of parameters involved in determining how long a merger signature will remain visible, it is plausible that several late-stage mergers could have been missed. Although a merger between gas rich galaxies can leave spectacular features for a long time, viewed from the wrong orientation they can be completely unnoticeable.

While it is difficult to asses the relevance for the timescale issue of major mergers being overlooked, we can be reasonably confident that the remnant will not look like a disk. Spheroidal and bulge-dominated galaxies are usually said to be formed as a result of major mergers (e.g., Toomre 1977; Barnes & Hernquist 1996; Cox et al. 2006). However, it has been also stated that disks can survive some major mergers, especially if the progenitors are gas-rich (e.g., Barnes & Hernquist 1996; Springel & Hernquist 2005; Hopkins et al. 2009), nonetheless these kind of mergers remnants have been argued to not lead to a large bulge growth and significant BH fueling (Hopkins & Hernquist 2009). Likewise, it has been argued that some gas-rich mergers can lead to the regrowth of the disk (Hopkins et al. 2009; Bundy et al. 2010). Even so, the timescales involved for such a process can be as much as an order of magnitude larger than the typical quasar lifetime of 1-100 Myr (e.g., Porciani et al. 2004; Hopkins et al. 2005b; Shen et al. 2007).

For the significant fraction of AGN hosted by disks found from our classification, we could safely say that the mechanism responsible for triggering those AGN was not a major merger, suggesting that since $z \sim 1$ alternative fueling methods seem to play a larger role than usually expected. Georgakakis et al. (2009), from a sample of X-ray selected AGN, compared the luminosity function of their disk-hosted AGN against the analytic model of the X-ray quasar luminosity function for a stochastic accretion mode by Hopkins & Hernquist (2006). They showed that the model can reproduce the observations, but at the same time the overall number density of the observed disks was underpredicted, especially at high X-ray luminosities. This suggests that alternative fueling methods (i.e., those that do not destroy the disk) are much more efficient than most existing models predict.

5.1.2. *No veiled X-ray activity in merging galaxies*

The aforementioned models leave the possibility that we could be missing an important fraction of AGN due to gas and dust obscuration when a gas-rich major merger is taking place. Even though obscured AGN can still be detected through their hard X-ray emission (Hopkins et al. 2005a), it is possible that less luminous and highly obscured AGN lie below the detection threshold used to build the X-ray catalogs (Treister et al. 2004). The X-ray properties of such obscured objects have been successfully studied in the literature by the means of a stacking analysis of X-ray data (e.g., Daddi et al. 2007; Fiore et al. 2009). If obscured AGN are being missed, they should be preferentially found in merging galaxies.

tensive case of the time lag scenario. They propose an all-merger driven AGN phase with a time lag of ∼500 Myr for their sample of early-type galaxies at $z \sim 0.05$. Even if their result is mainly based on the interpretation of their data as a causal sequence of events (and is subject to alternative explanations), they caution that their particular sample only accounts for a very small fraction (∼10%) of the overall AGN population found in the local universe.
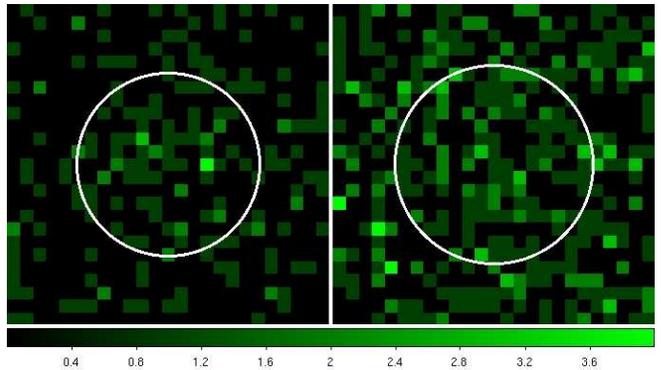
Figure 8. Stacked *Chandra* images of 45 inactive galaxies likely to be undergoing a major interaction, on the soft 0.5-2 keV (left) and hard 2-8 keV (right) energy bands, showing the average radii of the stacked sources as white circles. The cutouts are $12'' \times 12''$.

Therefore, in order to test this scenario and search for this potentially buried X-ray activity, we stack all the inactive galaxies regarded as highly distorted. 87 inactive galaxies fulfill our simultaneous criteria of being individually classified as either Dist-1 or Dist-2 with an agreement of $\geq 75\%$, and classified as Dist-2 with an agreement $\geq 65\%$.

For this analysis, we take advantage of the higher sensitivity of the *Chandra* observations of the COSMOS field (C-COSMOS, Elvis et al. 2009), compared with the *XMM-Newton* data. Even though *Chandra* covered only half of the field (~ 0.9 deg^2), it has a flux limit three times below the *XMM-Newton* sensitivity, which makes the tradeoff in smaller coverage absolutely justifiable, considering that we want to detect possible X-ray sources below the XMM-COSMOS catalog sensitivity threshold.

For the stacking of the X-ray data, we used the CSTACK tool[7] developed by one of the authors (TM), which includes a detailed bootstrapping error analysis through 500 realizations. Because the stacking is made from multiple observations, we consider the counts within a radius varying according to the off-axis angle, corresponding to 90% of the encircled counts. We stacked the 45 objects that lie within the C-COSMOS area, excluding 1 object that was close to an X-ray source. We found an excess of soft 0.5-2 keV and hard 2-8 keV count rates from the source region at modest levels of 2.2σ and 2.4σ respectively. Fig 8 shows the results of the stacking in the two energy bands, with the average radii of $3\rlap{.}''4$ and $3\rlap{.}''7$ for comparison, within which no source is noticeable above the background level.

The lack of any obvious source after the stacking suggests that this moderate excess could be due to either extended source emission (e.g., from a galaxy group), or from a few sources dominating the count rate lying at large off-axis angles from the *Chandra* image. Therefore, it is unlikely that we are missing a significant fraction of accreting BHs, hidden within the population of inactive galaxies undergoing interactions.

5.1.3. *No enhanced soft X-ray absorption in merging AGN host galaxies*

As mentioned before, AGN obscuration due to the surrounding gas and dust during a major merger would affect mainly the soft X-ray energy band, while the hard

[7] http://cstack.ucsd.edu

band would remain unobscured. If we observe an AGN hosted by a merging galaxy, and this interaction was responsible for the BH activity, we would expect to observe a hard X-ray spectrum from this source. To trace the obscuration level of our interacting AGN host galaxies, we compute their X-ray hardness ratio (HR). The HR is defined as

$$HR = (H - S)/(H + S), \qquad (4)$$

where H and S stand for to the hard (2-10 keV) and soft (0.5-2 keV) counts respectively. At our redshift range, it is still safe to say that HR values lower than -0.2 correspond to an unabsorbed, soft spectrum (Hasinger 2008).

From our visual analysis, we have 13 AGN host galaxies regarded as highly distorted with high agreement according to the criteria used before. By computing the HR for these objects, we find that, contrary to what models predict, all of these particular sources present soft X-ray spectra. All of them have HR values $\leq$-0.2, with a mean of -0.53, which shows a low attenuation in the soft band.

It has been argued, however, that the HR diagnostic is rather crude in terms of predicting obscuration, and indeed, bright Compton-thick AGN can feature soft X-ray spectra due to photoionized gas (Levenson et al. 2006). Even so, this is only valid when the AGN is not observed directly, and we can easily establish that at least for the type–1 sample this would not the case, and that we are certainly looking at active, accreting BHs. Looking *only* at the type–1 objects from these likely merging galaxies, we find that the average HR is -0.48 which indeed suggests a low level of obscuration.

One possible interpretation is that these interactions are not related to the observed AGN episode, and that are instead only chance encounters. Dissipationless or gas poor mergers could account for the lack of obscuration, but then it is unlikely that any strong merging signatures and substantial accretion onto the central BH would take place directly due to these kind of events. Pierce et al. (2007) found the same result for X-ray-selected AGN hosted by interacting galaxies, suggesting that the observed interactions were not responsible for the fueling of those accreting BHs.

From another perspective, however, the models mentioned earlier are limited by the proposed picture of the merger-ULIRG-feedback-quasar timeline (e.g., Sanders et al. 1988a,b; Hopkins et al. 2008), which is already regarded as oversimplified. The quasar phase is said to happen after coalescence, but observations of large samples of ULIRGs, all of them undergoing interactions, have found a significant scatter in the trends of AGN contribution, accretion rate, and dust obscuration with merging state (Veilleux et al. 2009). Some of these have even been found to be dominated by the AGN in pre-merging state. Chaotic behavior during a merger event can account for various unpredictable episodes of starburst and nuclear activity. Such episodic behavior, which can start much earlier than the final coalescence, can perfectly explain the soft spectra found in our interacting active galaxies, and at the same time go against the alternative time lag scenario.

5.2. *Major merging: not the most relevant mechanism*

Our analysis has demonstrated that the scenario in which mergers are responsible for triggering AGN after

a significant time lag is unlikely. The high fraction of disks, the lack of a hidden AGN signal in merging inactive galaxies, and the missing soft X-ray obscuration of interacting AGN hosts all appear to rule out this model as a possible explanation of our results. The absence of any further evidence in support of this scenario leads us to the only remaining possible interpretation of our results: active galaxies are involved in major mergers no more frequently than inactive galaxies, and mergers have not played a leading role in AGN triggering for the last 7.5 Gyr. Our results agree with the few recent studies that *have* used a control sample (Dunlop et al. 2003; Grogin et al. 2003, 2005; Pierce et al. 2007; Gabor et al. 2009; Reichard et al. 2009; Tal et al. 2009), in the sense that the morphologies of the AGN host galaxies are not unusual and do not show a preference for merging systems. Of the studies mentioned earlier which supported a merger-AGN connection, many only provided circumstantial evidence for such a link, without any control sample comparisons.

The lack of enhancement on merging signatures for AGN hosts with respect to the background level indicates that there is no causal connection between merging and AGN triggering up to $z \sim 1$ and $M_* \sim 10^{11.7} M_\odot$, the galaxies dominating BH growth at these redshifts. It is still a plausible scenario that major mergers could be responsible for some of the brightest quasars; we do not intend to neglect this possibility, but in the context of a clean, large X-ray selected population of AGN, it is certainly not the most relevant mechanism. The large fraction of AGN hosted by disk dominated galaxies shows that alternative mechanisms such as stochastic processes and minor mergers dominate for this sample of objects.

The merger-starburst connection has also been widely studied in the same perspective. Both mechanisms share the need for enough cold gas to be brought to the central regions of the galaxy, so it is worth mentioning analogous conclusions from the recent literature: (1) Indeed, major mergers *can* trigger strong starbursts (e.g., Mihos & Hernquist 1996; Springel 2000), but (2) *not always*, as seen in models (Di Matteo et al. 2007) and observations (Bergvall et al. 2003), and (3) its overall contribution is relatively modest (Di Matteo et al. 2008; Jogee et al. 2009), with no more than 10% of star formation in massive galaxies being triggered by major mergers at $z \sim 0.6$ (Robaina et al. 2009).

Hasinger (2008), by studying the absorption properties of X-ray selected AGN, proposed a scenario in which the major merger-driven evolution dominates early in the universe, producing the bulk of the brightest quasars at $z = 2-3$. Later, around $z \sim 1$, secular evolution and minor interactions take the lead, becoming the main fueling mechanisms. While we cannot perform the same analysis at higher redshifts with the current observational dataset, our results appear to fit this picture. Nevertheless, the overall relevance of major merging, even in the early universe, has yet to be determined. Recent studies suggest that secular processes play a much larger role: observations of massive star-forming galaxies at $z \sim 2$ have shown that their build up has been dominated by cold rapid accretion and secular processes (Genzel et al. 2008), without the need of major mergers. It has been stated on the basis of dark matter simulations that the likely number of major mergers is insufficient to account

for the transformation of star-forming turbulent disks at $z = 2$ into ellipticals at $z = 0$ (Genel et al. 2008). A broader view of the accretion history of dark matter halos by Genel et al. (2010), quantified that $\sim 60\%$ of the dark matter in a given halo is contributed by mergers, with only $\sim 20\%$ being major mergers. Instead, the rest ($\sim 40\%$) of the dark matter would be accreted smoothly. Furthermore, this also agrees with recent work using smooth particle hydrodynamics simulations, stating that galaxies have acquired most of their baryonic mass through the 'cold mode' of accretion (Kereš et al. 2005, 2009). Even though these studies have not addressed the BH buildup problem specifically, they have shown that secular processes can be highly relevant at the redshifts at which the peak of quasar activity occurs.

6. CONCLUSIONS

In this work we performed a consistent visual analysis on the *HST*-based morphologies of a sample of 140 X-ray selected AGN host galaxies over $z \sim 0.3 - 1.0$ and $M_* < 10^{11.7} M_\odot$, and compared them with a matched control sample of inactive galaxies under the same conditions. Our goal was to search for the presence of any significant connection between major merging and BH fueling as suggested by models and observational tests. In summary:

1. From our visual analysis, $\sim 85\%$ of our AGN host galaxies show no strong distortions on their morphologies. Comparison with the control sample shows that the distortion fractions are equal within the 68% central confidence level. Given our sample size, we can state that at a 95% confidence level the highly distorted fraction of AGN hosts is less than 1.9 times that of the inactive galaxies. Mergers and interactions involving AGN hosts are not dominant, and occur no more frequently than for inactive galaxies.

2. Over 50% of the AGN from our sample are hosted by disk dominated galaxies, implying a triggering mechanism that would not destroy the disk, i.e.,

not a major merger. This also indicates that it is unlikely that we could be missing major mergers due to strong distortions having already been washed out over a large time lag prior to the ignition of the AGN.

3. Through a detailed stacking analysis of the X-ray data of our inactive galaxies undergoing mergers, we did not find an underlying X-ray signal indicating the presence of a substantial population of obscured AGN.

4. Looking at the hardness of the X-ray emission of our AGN hosts that are clearly undergoing an interaction, we found soft X-ray spectra in all of them, contradicting the expected obscuration in this band predicted by models. This can either be because either the observed interactions are not resposible for the AGN fueling, or that the unpredictable output of a merger event allows many accretion phases even during such early stages.

Our work explicitly suggests that, at least for the last 7.5 Gyr, major merging has not been the most relevant mechanism in the triggering of typical AGN, and that the bulk of the BH accretion occurs through secular processes and minor interactions. The alternative interpretation of a time lag between merger trigger and AGN onset is unlikely due to the zero enhancement of the distortion fraction, the high incidence of disks, and complete absence of any obscured AGN signal on ongoing merging galaxies without an X-ray detection.

APPENDIX

A. QUASAR-HOST GALAXY DECOMPOSITION

The light distribution of the type–1 AGN is clearly dominated by the quasar, and because we want to analyze the morphologies of their host galaxies, accurate removal of the bright nucleus is of vital importance. This is done through a rigorous two-dimensional parametric fitting with GALFIT, with which we reduce each system down to a two-component model: a point spread function (PSF) to represent the AGN, and a Sérsic light profile accounting for the host galaxy. After subtraction of the modeled PSF, we are left with the host galaxy emission plus some residuals. Previous simulations have shown that, at our resolution and S/N, it is sufficient with a single-component model to account for the host galaxy rather than a more complex, multi-component one (Sánchez et al. 2004; Simmons & Urry 2008).

An appropriate initial guess of the parameters is recommended to get a faster and converging model with GALFIT. We opt to run Source Extractor (Bertin & Arnouts 1996) on our cutouts to generate, in a fast and automatic way, rough estimates of the free parameters of the Sérsic profile, such as coordinates within the image, observed magnitude, axis-ratio b/a, half-light radius R_e, and position angle.

To ensure a reliable decomposition, we take particular care that the host galaxy is modeled with the least possible unnecessary flux transfer between PSF and the Sérsic profile, which would result in either an over- or undersubtraction. We perform several GALFIT runs on each object with 3 different choices for the Sérsic index n: we fix it to a $n=1$ exponential profile (Freeman 1970), to a $n=4$ de Vaucouleurs (1948) profile, and we also leave it a as free parameter for GALFIT to decide. To choose the right model, we need our best fit to be reasonable in terms of the resulting parameters. We require our host galaxy model: (1) not to be too concentrated or too shallow, meaning a half-light radius between 2.5 pixels $< R_e <$ 100 pixels, (2) not to diverge to extreme elongations, therefore to have $b/a > 0.5$,
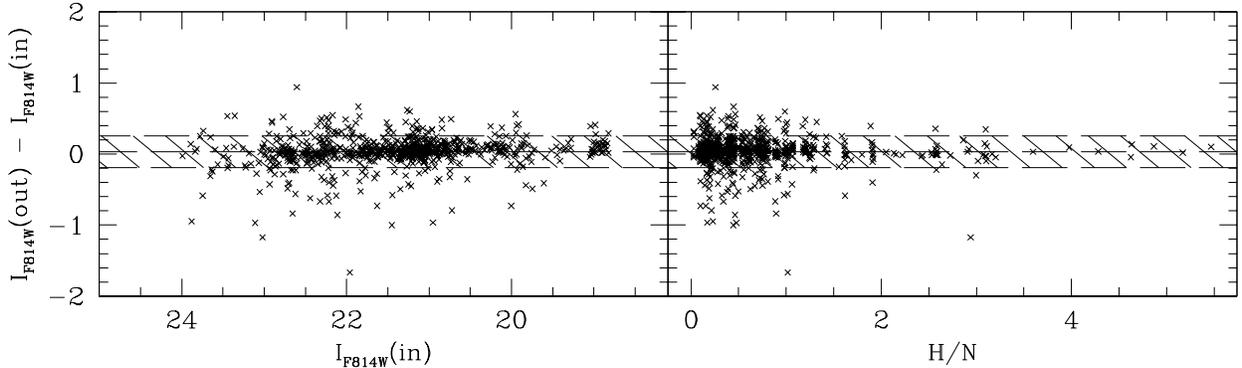
Figure 9. The difference in the observed magnitudes (I_{F814W}) of the comparison galaxies before (in) and after (out) the point source addition/subtraction. The left-hand panel plots this difference against the initial magnitude, and the right-hand panel against the host to nucleus flux ratio, H/N. The 1σ deviation away from the mean is 0.23 mag, indicated by the shaded area centered at 0.03 mag.

and (3) to have its Sérsic index within $0.5 < n < 8$, for the free n case. We interpret that if the values run away from these boundaries, GALFIT did not manage to model the underlying galaxy but instead could be accounting for uncertainties in the PSF.

A key aspect of the AGN–host galaxy decomposition is the choice of an accurate PSF, both for modeling the AGN itself and for deconvolving the host galaxy light distribution. Even though the space-based *HST* provides extremely precise PSFs, instrumental effects are still important. The position of the target within the detector and the temporal variability along different orbits can lead to discrepancies between the PSFs from the observations and the ones used for the analysis. This yields systematic errors in the image decomposition which can be critical for very bright AGN. The COSMOS survey provides us with the opportunity to minimize these spatial and temporal effects by using stellar PSFs from stars observed under the same conditions than our targets. For each object, we build specific PSFs by averaging the nearest $\sim$30 stars in the same manner to other similar studies with large *HST* coverage (Jahnke et al. 2004; Sánchez et al. 2004). The *rms* error from the creation of each PSF is propagated to the intrinsic variance of the AGN; the uncertainty of the object being fitted is required by GALFIT in order to converge to a minimum normalized χ^2.

B. CREATING MOCK AGN HOSTS

We build a sample of simulated AGN by adding stars as fake nuclei to our inactive galaxies. To remain true to the characteristic blue colors of the AGN, we perform an initial selection of stars from the COSMOS ACS archive by placing color cuts in $(B - V) < 0.75$ and $(V - R) < 0.95$. For each of the control galaxies, we look for stars that match the contrast level between the fluxes of the host and nucleus (H/N) of the corresponding AGN. With a matching star found, we simply add it over the centroid of the galaxy.

We then apply the same point source removal procedure as for the original AGN sample. PSFs are created exactly as before, and the light contributions of the star and the underlying galaxy are separated using GALFIT. With the exception of 3 unsuccessful fits, we are left with 732 simulated AGN host galaxies.

C. TESTING THE RELIABILITY OF THE IMAGE DECOMPOSITION

The creation of a sample of simulated AGN-subtracted hosts from a starting point of real galaxies and stars gives us the opportunity to check the impact of our nucleus removal technique, and to see whether this technique is biased. How significant are the residuals? We have performed photometry on the control galaxies before and after the addition/subtraction of the fake nucleus. If a large magnitude offset were to be found, we would have had to consider reselecting our control sample, because we would inevitably be comparing active and inactive galaxies with different observed magnitudes. We find that, on average, the galaxies are fainter by 0.03 mag after the subtraction, with a 1σ deviation of 0.23 mag. Figure 9 shows the difference between the initial and recovered magnitudes for the hosts as a function of the initial magnitudes and H/N ratio for our control galaxies. There is no obvious correlation between the offset and the initial magnitudes of the galaxies, but as expected the recovered values tend to be less exact for more compact galaxies and brighter active nuclei.

These results show that this technique is trustworthy, and the offset found can be considered negligible and does not affect our choice of a comparison sample.

REFERENCES

Bahcall, J. N., Kirhakos, S., Saxe, D. H., & Schneider, D. P. 1997, ApJ, 479, 642
Barnes, J. E., & Hernquist, L. 1996, ApJ, 471, 115
Barnes, J. E., & Hernquist, L. E. 1991, ApJ, 370, L65
Bell, E. F., & de Jong, R. S. 2001, ApJ, 550, 212

Bell, E. F., Phleps, S., Somerville, R. S., Wolf, C., Borch, A., & Meisenheimer, K. 2006, ApJ, 652, 270
Bennert, N., Canalizo, G., Jungwiert, B., Stockton, A., Schweizer, F., Peng, C. Y., & Lacy, M. 2008, ApJ, 677, 846
Bergvall, N., Laurikainen, E., & Aalto, S. 2003, A&A, 405, 31
Bertin, E., & Arnouts, S. 1996, A&AS, 117, 393
Brusa, M., et al. 2007, ApJS, 172, 353
—. 2010, ApJ, 716, 348

Bundy, K., et al. 2010, ApJ, 719, 1969

Canalizo, G., Bennert, N., Jungwiert, B., Stockton, A., Schweizer, F., Lacy, M., & Peng, C. 2007, ApJ, 669, 801

Canalizo, G., & Stockton, A. 2000, AJ, 120, 1750

—. 2001, ApJ, 555, 719

Capak, P., et al. 2007, ApJS, 172, 99

Cappelluti, N., et al. 2009, A&A, 497, 635

Cole, S., Lacey, C. G., Baugh, C. M., & Frenk, C. S. 2000, MNRAS, 319, 168

Cox, T. J., Jonsson, P., Primack, J. R., & Somerville, R. S. 2006, MNRAS, 373, 1013

Cox, T. J., Jonsson, P., Somerville, R. S., Primack, J. R., & Dekel, A. 2008, MNRAS, 384, 386

Daddi, E., et al. 2007, ApJ, 670, 173

de Vaucouleurs, G. 1948, Annales d'Astrophysique, 11, 247

Di Matteo, P., Bournaud, F., Martig, M., Combes, F., Melchior, A., & Semelin, B. 2008, A&A, 492, 31

Di Matteo, P., Combes, F., Melchior, A., & Semelin, B. 2007, A&A, 468, 61

Di Matteo, T., Springel, V., & Hernquist, L. 2005, Nature, 433, 604

Dunlop, J. S., McLure, R. J., Kukula, M. J., Baum, S. A., O'Dea, C. P., & Hughes, D. H. 2003, MNRAS, 340, 1095

Elvis, M., et al. 2009, ApJS, 184, 158

Ferrarese, L., & Merritt, D. 2000, ApJ, 539, L9

Fiore, F., et al. 2009, ApJ, 693, 447

Freeman, K. C. 1970, ApJ, 160, 811

Gabor, J. M., et al. 2009, ApJ, 691, 705

Gebhardt, K., et al. 2000, ApJ, 539, L13

Gehren, T., Fried, J., Wehinger, P. A., & Wyckoff, S. 1984, ApJ, 278, 11

Genel, S., Bouché, N., Naab, T., Sternberg, A., & Genzel, R. 2010, ApJ, 719, 229

Genel, S., et al. 2008, ApJ, 688, 789

Genzel, R., et al. 2008, ApJ, 687, 59

Georgakakis, A., et al. 2009, MNRAS, 397, 623

Giavalisco, M., et al. 2004, ApJ, 600, L93

Granato, G. L., De Zotti, G., Silva, L., Bressan, A., & Danese, L. 2004, ApJ, 600, 580

Grogin, N. A., et al. 2003, ApJ, 595, 685

—. 2005, ApJ, 627, L97

Gunn, J. E. 1979, in Active Galactic Nuclei, 213–225

Häring, N., & Rix, H. 2004, ApJ, 604, L89

Hasinger, G. 2008, A&A, 490, 905

Hasinger, G., et al. 2007, ApJS, 172, 29

Heckman, T. M., Bothun, G. D., Balick, B., & Smith, E. P. 1984, AJ, 89, 958

Hernquist, L. 1989, Nature, 340, 687

Hopkins, P. F., Cox, T. J., Younger, J. D., & Hernquist, L. 2009, ApJ, 691, 1168

Hopkins, P. F., & Hernquist, L. 2006, ApJS, 166, 1

—. 2009, ApJ, 694, 599

Hopkins, P. F., Hernquist, L., Cox, T. J., Di Matteo, T., Martini, P., Robertson, B., & Springel, V. 2005a, ApJ, 630, 705

Hopkins, P. F., Hernquist, L., Cox, T. J., & Kereš, D. 2008, ApJS, 175, 356

Hopkins, P. F., Hernquist, L., Cox, T. J., Robertson, B., & Krause, E. 2007, ApJ, 669, 45

Hopkins, P. F., Hernquist, L., Martini, P., Cox, T. J., Robertson, B., Di Matteo, T., & Springel, V. 2005b, ApJ, 625, L71

Hutchings, J. B., Crampton, D., Campbell, B., Duncan, D., & Glendenning, B. 1984, ApJS, 55, 319

Hutchings, J. B., Johnson, I., & Pyke, R. 1988, ApJS, 66, 361

Hutchings, J. B., & Neff, S. G. 1992, AJ, 104, 1

Ilbert, O., et al. 2009, ApJ, 690, 1236

—. 2010, ApJ, 709, 644

Jahnke, K., & Maccio, A. 2010, ArXiv e-prints

Jahnke, K., et al. 2004, ApJ, 614, 568

Jogee, S. 2006, in Lecture Notes in Physics, Berlin Springer Verlag, Vol. 693, Physics of Active Galactic Nuclei at all Scales, ed. D. Alloin, 143–+

Jogee, S., et al. 2009, ApJ, 697, 1971

Kauffmann, G., & Haehnelt, M. 2000, MNRAS, 311, 576

Kauffmann, G., White, S. D. M., & Guiderdoni, B. 1993, MNRAS, 264, 201

Kereš, D., Katz, N., Fardal, M., Davé, R., & Weinberg, D. H. 2009, MNRAS, 395, 160

Kereš, D., Katz, N., Weinberg, D. H., & Davé, R. 2005, MNRAS, 363, 2

Koekemoer, A. M., et al. 2007, ApJS, 172, 196

Kormendy, J., & Richstone, D. 1995, ARA&A, 33, 581

Leauthaud, A., et al. 2007, ApJS, 172, 219

Levenson, N. A., Heckman, T. M., Krolik, J. H., Weaver, K. A., & Życki, P. T. 2006, ApJ, 648, 111

Lilly, S. J., et al. 2007, ApJS, 172, 70

Lin, L., et al. 2008, ApJ, 681, 232

Lintott, C. J., et al. 2008, MNRAS, 389, 1179

Lotz, J. M., Jonsson, P., Cox, T. J., & Primack, J. R. 2008, MNRAS, 391, 1137

Lusso, E., et al. 2010, A&A, 512, A34+

Lynden-Bell, D. 1967, MNRAS, 136, 101

Magorrian, J., et al. 1998, AJ, 115, 2285

Mainieri, V., et al. 2007, ApJS, 172, 368

Marconi, A., & Hunt, L. K. 2003, ApJ, 589, L21

Martini, P. 2004, in IAU Symposium, Vol. 222, The Interplay Among Black Holes, Stars and ISM in Galactic Nuclei, ed. T. Storchi-Bergmann, L. C. Ho, & H. R. Schmitt, 235–241

Mihos, J. C., & Hernquist, L. 1996, ApJ, 464, 641

Peng, C. Y. 2007, ApJ, 671, 1098

Peng, C. Y., Ho, L. C., Impey, C. D., & Rix, H. 2010, AJ, 139, 2097

Peng, C. Y., Ho, L. C., Impey, C. D., & Rix, H.-W. 2002, AJ, 124, 266

Pierce, C. M., et al. 2007, ApJ, 660, L19

Porciani, C., Magliocchetti, M., & Norberg, P. 2004, MNRAS, 355, 1010

Ramos Almeida, C., Tadhunter, C. N., Inskip, K. J., Morganti, R., Holt, J., & Dicken, D. 2010, ArXiv e-prints

Reichard, T. A., Heckman, T. M., Rudnick, G., Brinchmann, J., Kauffmann, G., & Wild, V. 2009, ApJ, 691, 1005

Richstone, D., et al. 1998, Nature, 395, A14+

Rix, H., et al. 2004, ApJS, 152, 163

Robaina, A. R., Bell, E. F., van der Wel, A., Somerville, R. S., Skelton, R. E., McIntosh, D. H., Meisenheimer, K., & Wolf, C. 2010, ApJ, 719, 844

Robaina, A. R., et al. 2009, ApJ, 704, 324

Salvato, M., et al. 2009, ApJ, 690, 1250

Sánchez, S. F., et al. 2004, ApJ, 614, 586

Sanders, D. B., & Mirabel, I. F. 1996, ARA&A, 34, 749

Sanders, D. B., Soifer, B. T., Elias, J. H., Madore, B. F., Matthews, K., Neugebauer, G., & Scoville, N. Z. 1988a, ApJ, 325, 74

Sanders, D. B., Soifer, B. T., Elias, J. H., Neugebauer, G., & Matthews, K. 1988b, ApJ, 328, L35

Scarlata, C., et al. 2007, ApJS, 172, 406

Schawinski, K., Dowlin, N., Thomas, D., Urry, C. M., & Edmondson, E. 2010, ApJ, 714, L108

Scoville, N., et al. 2007a, ApJS, 172, 38

—. 2007b, ApJS, 172, 1

Sersic, J. L. 1968, Atlas de galaxias australes, ed. J. L. Sersic

Shen, Y., et al. 2007, AJ, 133, 2222

Simkin, S. M., Su, H. J., & Schwarz, M. P. 1980, ApJ, 237, 404

Simmons, B. D., & Urry, C. M. 2008, ApJ, 683, 644

Soltan, A. 1982, MNRAS, 200, 115

Somerville, R. S., Hopkins, P. F., Cox, T. J., Robertson, B. E., & Hernquist, L. 2008, MNRAS, 391, 481

Somerville, R. S., Primack, J. R., & Faber, S. M. 2001, MNRAS, 320, 504

Springel, V. 2000, MNRAS, 312, 859

Springel, V., Di Matteo, T., & Hernquist, L. 2005, MNRAS, 361, 776

Springel, V., & Hernquist, L. 2005, ApJ, 622, L9

Stockton, A. 1982, ApJ, 257, 33

Stockton, A., & Ridgway, S. E. 1991, AJ, 102, 488

Surace, J. A., & Sanders, D. B. 1999, ApJ, 512, 162

Surace, J. A., Sanders, D. B., & Evans, A. S. 2000, ApJ, 529, 170

Surace, J. A., Sanders, D. B., Vacca, W. D., Veilleux, S., & Mazzarella, J. M. 1998, ApJ, 492, 116

Tal, T., van Dokkum, P. G., Nelan, J., & Bezanson, R. 2009, AJ, 138, 1417

Taniguchi, Y. 1999, ApJ, 524, 65

Toomre, A. 1977, in Evolution of Galaxies and Stellar Populations, ed. B. M. Tinsley & R. B. Larson, 401

Toomre, A., & Toomre, J. 1972, ApJ, 178, 623
Treister, E., et al. 2004, ApJ, 616, 123
Tremaine, S., et al. 2002, ApJ, 574, 740
Trump, J. R., et al. 2007, ApJS, 172, 383
—. 2009, ApJ, 696, 1195
Urrutia, T., Lacy, M., & Becker, R. H. 2008, ApJ, 674, 80

van der Wel, A., Rix, H., Holden, B. P., Bell, E. F., & Robaina,
    A. R. 2009, ApJ, 706, L120
Veilleux, S., et al. 2009, ApJS, 182, 628
Volonteri, M., Haardt, F., & Madau, P. 2003, ApJ, 582, 559
Wada, K. 2004, Coevolution of Black Holes and Galaxies, 186
Wyithe, J. S. B., & Loeb, A. 2003, ApJ, 595, 614
Yu, Q., & Tremaine, S. 2002, MNRAS, 335, 965
Zakamska, N. L., et al. 2006, AJ, 132, 1496